© 2014. Published by The Company of Biologists Ltd | Development (2014) 141, 2150-2156 doi:10.1242/dev.107011

RESEARCH ARTICLE

Scaling morphogen gradients during tissue growth by a cell division rule

Inna Averbukh[1,*], Danny Ben-Zvi[2,*], Siddhartha Mishra[3,4,*] and Naama Barkai[1,‡]

ABSTRACT

Morphogen gradients guide the patterning of tissues and organs during the development of multicellular organisms. In many cases, morphogen signaling is also required for tissue growth. The consequences of this interplay between growth and patterning are not well understood. In the *Drosophila* wing imaginal disc, the morphogen Dpp guides patterning and is also required for tissue growth. In particular, it was recently reported that cell division in the disc correlates with the temporal increase in Dpp signaling. Here we mathematically model morphogen gradient formation in a growing tissue, accounting also for morphogen advection and dilution. Our analysis defines a new scaling mechanism, which we term the morphogen-dependent division rule (MDDR): when cell division depends on the temporal increase in morphogen signaling, the morphogen gradient scales with the growing tissue size, tissue growth becomes spatially uniform and the tissue naturally attains a finite size. This model is consistent with many properties of the wing disc. However, we find that the MDDR is not consistent with the phenotype of scaling-defective mutants, supporting the view that temporal increase in Dpp signaling is not the driver of cell division during late phases of disc development. More generally, our results show that local coupling of cell division with morphogen signaling can lead to gradient scaling and uniform growth even in the absence of global feedbacks. The MDDR scaling mechanism might be particularly beneficial during rapid proliferation, when global feedbacks are hard to implement.

KEY WORDS: Dpp, *Drosophila*, Growth, Morphogen, Scaling, Wing disc

INTRODUCTION

Individuals of the same species vary in size due to environmental, genetic and stochastic fluctuations. The body plan remains robust to size variations, in part owing to mechanisms that function at early development to adjust (scale) the pattern of the developing tissue with its size. Scaling entails an effective transmission of global size information to the local setting of each cell. Proposed scaling mechanisms include opposing molecular gradients emanating from opposite poles and dilution of some molecular component defining the morphogen length scale (Wartlick et al., 2011). Most of these theoretical scaling mechanisms assume that tissue pattern is adjusted with tissue size, while size itself is defined independently of the patterning process (Barkai and Ben-Zvi, 2009; Ben-Zvi et al., 2008; Cheung et al., 2011; Gierer and Meinhardt, 1972; Gregor et al., 2008; Houchmandzadeh et al., 2002; Patel and Lall, 2002; Wolpert, 1969). Yet patterning is often concomitant with tissue growth. Furthermore, the same molecules that guide patterning may also be required for tissue proliferation, directly coupling pattern and size (Lanctot et al., 2013; Sato and Kornberg, 2002; Towers et al., 2008). How global tissue properties such as pattern scaling and tissue growth are affected by this local coupling is not well understood.

The *Drosophila* wing imaginal disc provides a central model for studying both pattern scaling and the coordination of patterning and growth. This monolayer epithelium is patterned along the anterior-posterior (AP) axis by a concentration gradient of the Bmp4 homolog Dpp, which is secreted from a line-like source along the AP border and decays gradually away from it (Kicheva et al., 2007). The Dpp concentration gradient was directly visualized and shown to scale with the size of the disc when disc size was perturbed by genetic mutations, and also during the growth of the wild-type disc (Ben-Zvi et al., 2011a; Hamaratoglu et al., 2011; Teleman and Cohen, 2000; Wartlick et al., 2011). Recent results by several groups (including ours) suggest that Dpp gradient scaling depends on expansion-repression (ExR) feedback, in which a diffusible 'expander' molecule that facilitates the spread of the morphogen is repressed by morphogen signaling (Ben-Zvi and Barkai, 2010) (Fig. 1A,B). The secreted molecule Pentagone (Magu – FlyBase) acts as an expander: it is widely diffusible, facilitates the spread of Dpp in a non-cell-autonomous manner and its production is repressed by Dpp signaling (Vuilleumier et al., 2011). Indeed, scaling was lost in third instar wing discs of *pentagone* null mutants, or when its expression was constitutive throughout the disc (Ben-Zvi et al., 2011a, b; Hamaratoglu et al., 2011; Restrepo and Basler, 2011).

In addition to its role as a morphogen patterning the wing disc, Dpp is a growth factor required for the proliferation of cells in the disc (reviewed by Affolter and Basler, 2007; Schwank and Basler, 2010). Interestingly, although Dpp levels decay along the disc, cell proliferation is spatially homogenous (Milan et al., 1996). This spatially uniform growth may be beneficial for reducing mechanical stress (Shraiman, 2005) and for increasing patterning robustness (Schwank and Basler, 2010). Different models were suggested to explain how a graded morphogen profile can direct uniform tissue growth. One proposal is that growth depends on the relative slope of morphogen concentration, which remains position-independent for exponentially decaying gradients (Day and Lawrence, 2000; Rogulja and Irvine, 2005); however, this model cannot explain growth within or at the borders of clones with uniform Dpp signaling (Schwank et al., 2008). Others have proposed that cell division is influenced by mechanical forces that depend on morphogen signaling but spread uniformly along the tissue (Aegerter-Wilmsen et al., 2007; Hufnagel et al., 2007; Shraiman, 2005). Notably, growth of the disc is regulated by additional pathways including Wg and Hippo signaling (Johnston and Sanders, 2003; Rogulja et al., 2008), and by systemic signals such as insulin-like growth factors (Bohni et al., 1999). These signals could

[1]Department of Molecular genetics, Weizmann Institute of Science, Rehovot 76100, Israel. [2]Department of Stem Cell and Regenerative Biology, Harvard University, Cambridge, MA 02138, USA. [3]Center of Mathematics for Applications, University of Oslo, 0316 Oslo, Norway. [4]Seminar for Applied Mathematics ETH, Zurich 8092, Switzerland.
*These authors contributed equally to this work

‡Author for correspondence (naama.barkai@weizmann.ac.il)

Received 11 December 2013; Accepted 26 March 2014

Development (2014) 141, 2150-2156 doi:10.1242/dev.107011

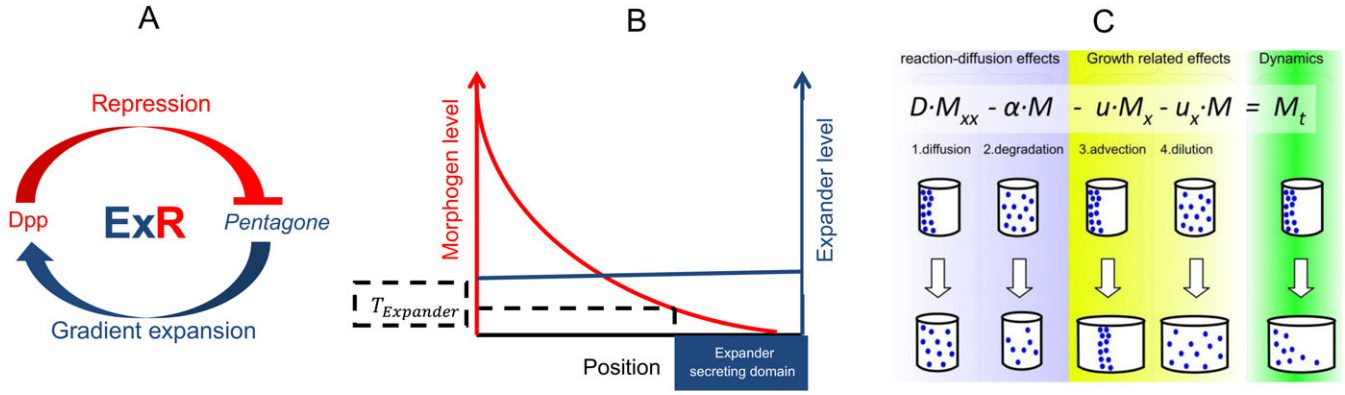

Fig. 1. ExR and coupling growth and patterning by a morphogen. (A) The expansion-repression (ExR) feedback topology. The morphogen represses the secretion of an expander. The expander, which is diffusible and stable, expands the morphogen gradient by enhancing morphogen diffusion and/or decreasing morphogen degradation. (B) Expansion of the morphogen gradient leads to the gradual restriction of the expander secretion domain towards the distal region of the tissue. $T_{Expander}$ is the threshold for expander production repression. The gradient continues to expand until the expander is repressed almost throughout the entire field. The expander accumulates during the expansion of the gradient, such that larger fields will require higher levels of the expander. (C) Morphogen dynamics in a growing tissue. Coupling between growth and patterning by a morphogen gradient. The morphogen gradient profile is determined by morphogen diffusion (1) and its degradation (2). Owing to growth, two other terms shape the distribution: advection of the morphogen (3) and its dilution (4).

compensate for the graded distribution of Dpp to account for uniform growth (Schwank et al., 2011).

Dpp signaling and cell division rates have been quantified *in vivo* in the growing wing disc. The division cycle was shown to strongly correlate with the temporal increase in Dpp signaling, such that cells divided when Dpp signaling increased by ~50% relative to its level at the beginning of the division cycle (Wartlick et al., 2011). This correlation might suggest that cell division is defined by this temporal increase in Dpp signaling. Wartlick et al. noted that such a division rule could lead to spatially uniform growth, provided that the Dpp gradient scales with disc size through some external mechanism.

An emerging idea is, therefore, that the ExR mechanism functions to scale the Dpp gradient with the size of the growing disc, while the Dpp-dependent growth rule described above ensures spatially uniform growth. We examined the consistency of this proposal and were particularly interested in two aspects of this combined dynamics. First, the ExR feedback is effective in scaling morphogen gradients during slow growth, which gives the expander sufficient time to spread in the tissue, but becomes less effective when growth is rapid and the expander does not have time to diffuse and affect the entire tissue. We therefore studied the relation between morphogen gradient and disc size throughout the dynamics of disc growth, including early times when growth is rapid. Second, cells in the lateral domain of the disc receive very little if any Dpp signaling and express Brinker but proliferate at the same rate as medially located cells. Moreover, Brinker-expressing clones in the medial domain proliferate normally (Schwank et al., 2012). These observations led to a debate as to whether the correlation between cell division and the temporal increase in Dpp signaling seen in wild-type discs reflects a causal relationship (Schwank et al., 2012; Wartlick et al., 2012). We were interested in understanding qualitative properties of the proposed Dpp-dependent growth rule to evaluate its consistency with respect to different mutant backgrounds.

To this end, we simulated the ExR feedback in the growing disc using a mathematical framework that accounts for morphogen diffusion, advection and dilution during growth of the tissue. The morphogen-dependent division rule was incorporated into the dynamics, while other contributions to tissue growth were ignored, enabling us to focus exclusively on the properties of this proposed growth mechanism. Surprisingly, scaling and uniform growth were observed throughout the dynamics, also at early times when proliferation was too rapid for the ExR feedback to be effective. Extensive numerical analysis showed that scaling and uniform growth are intertwined at this stage and result solely from the dependence of cell division on the temporal increase in Dpp signaling. Prompted by this observation, we show analytically and numerically that this local MDDR mechanism can result in three global tissue properties: gradient scaling, uniform growth and a final size. We find that MDDR is consistent with many properties of wing disc growth. However, it cannot explain growth of the disc in *pentagone* null discs, in which scaling is lost in third instar, supporting the view that Dpp-independent factors contribute to growth of the disc at that time. More generally, our study demonstrates that local coupling of cell division with morphogen signaling may provide an efficient mechanism for establishing global pattern scaling and tissue growth properties, effective particularly under situations in which global feedbacks are harder to implement.

RESULTS

Model: simulating the ExR feedback in a growing tissue

We consider a one-dimensional growing tissue of size $[0,L(t)]$. The tissue consists of dividing cells whose division times $\tau(x,t)$ depend on time t and cell position x. Since cell division leads to tissue growth, each cell moves with a velocity $u(x,t)$ defined by the cell division rate (see methods in the supplementary material):

$$\frac{du}{dx} \equiv u_x \approx \frac{\ln(2)}{\tau(x,t)}. \quad (1)$$

Here, and in the following, u_x denotes the derivative of u with respect to x. We model a morphogen gradient that is established over the growing tissue. The morphogen with concentration M is secreted from the proximal edge ($x=0$), diffuses with some diffusion coefficient D_M, and degrades linearly at some rate α. To simulate the ExR feedback, we assume that the diffusion and/or degradation of the morphogen depend on some secreted molecule (the expander) with concentration E, the production of which is repressed by morphogen signaling. The expander is widely diffusible and is

Development (2014) 141, 2150-2156 doi:10.1242/dev.107011

degraded slowly. Using the Reynolds transport theorem, we can model the dynamics of the morphogen-expander system using advection-reaction-diffusion equations (Bittig, 2008) (see methods in the supplementary material):

$$M_t = D_M(E)\cdot M_{xx} - \alpha(E)\cdot M - u\cdot M_x - u_x\cdot M, \quad (2a)$$

$$E_t = D_E\cdot E_{xx} - \alpha_E\cdot E - u\cdot E_x - u_x\cdot E + \beta_E\cdot h(M). \quad (2b)$$

The first two terms on the right-hand sides of Eqn 2 describe the change in morphogen or expander concentration due to their respective diffusion and degradation. We assume that both secreted molecules are transported across the field by the movement of the underlying cells, to which they are weakly bound, e.g. through interaction with the extracellular matrix. This movement is described by the third (advection) term. Finally, growth of the tissue dilutes both morphogen and expander, thereby reducing their concentration. This dilution depends on the proliferation rate u_x and is accounted for by the fourth term (Fig. 1C). We assume a constant flux at the proximal boundary: $D_M M_x(L{=}0,t){=}{-}\eta$, zero morphogen flux at the distal boundary, and zero flux at both boundaries of the expander. β_E denotes the rate by which the expander is produced and $h(M){=}(1{+}(M/T_{rep})^n)^{-1}$ describes the morphogen-dependent repression of expander production, which is low at proximal regions where morphogen is high, and high at distal regions where morphogen concentration is low. Note that the region in which the expander is repressed increases as the morphogen expands. We also assume that the expander functions by limiting morphogen degradation, i.e. we set $\alpha(E){=}(\alpha_M/(1{+}E))$ and $D_M(E){=}D_M$ with α_M the morphogen degradation rate without the expander. The analysis is equivalent for assuming modulation of diffusion.

We began by simulating the temporal dynamics of the morphogen-expander distributions in discs growing at different, spatially uniform growth rates (supplementary material Fig. S1) and compared the scaling of the profile in the presence or absence of ExR feedback. As expected, ExR improved scaling at slow growth rates q, but was less effective in faster growing tissues (Ben-Zvi et al., 2011a; Hamaratoglu et al., 2011).

Simulating the Dpp gradient in a growing tissue

We next incorporated the growth rule implied by Wartlick and colleagues, whereby the cell divides when subject to a 50% increase in morphogen signaling (Wartlick et al., 2011). This division rule can be formulated as:

$$\tau(x,t)^{-1} = \theta^{-1}\frac{\dot{M}}{M}, \quad (3)$$

where $\dot{M}$ denotes the full (advective) derivative of M with respect to time, corresponding to the change in morphogen concentration as sensed by the moving cell, and $\theta{=}0.5$ is the fractional change in morphogen signaling required for triggering cell division. Together, Eqns 1-3 describe a closed system in which tissue growth and morphogen gradient formation are coupled.

We simulated this coupled system using parameters measured for the *Drosophila* wing imaginal disc (Fig. 2). The normalized morphogen profile scaled with the size of the growing tissue in accordance with experimental observations (Wartlick et al., 2011) (Fig. 2A,B,F). Growth began rapidly, but gradually slowed down asymptotically at a finite tissue size, comparable to the behavior observed in the wing imaginal disc (Wartlick et al., 2011) (Fig. 2D). Finally, cell division rate was practically independent of cell position along the tissue, consistent with the spatially uniform growth dynamics reported (Milan et al., 1996; Wartlick et al., 2011) (Fig. 2C). Notably, the proliferation rate was much smaller than the Dpp degradation rate throughout the dynamics (Fig. 2E).

We conclude that the coupled dynamics consisting of ExR feedback and MDDR is consistent with growth of the wild-type disc in at least three key aspects: scaling of the Dpp gradient with the size of the growing tissue, spatially uniform tissue growth, and

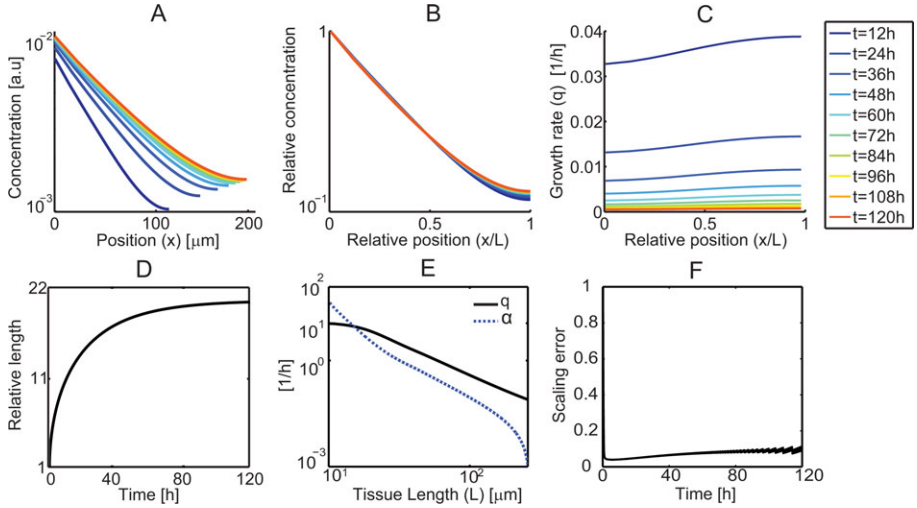

Fig. 2. Numerical simulation results for morphogen gradient dynamics in a tissue growing according to the MDDR with ExR feedback. Parameters correspond to reported measurements of third instar *Drosophila* wing imaginal disc (Wartlick et al., 2011). In all cases, we assume a constant morphogen flux from the source. (A) Morphogen level as a function of position in the tissue at various times. (B) Relative morphogen level as a function of relative position in the tissue. Overlap of the profiles indicates scaling of morphogen gradient with size. (C) Proliferation rate at various times as a function of relative position. Growth is spatially uniform and its rate declines with time. (D) Fold change increase in tissue size as a function of time. (E) Effective morphogen degradation rate α (dotted blue line) and growth rate $q{=}\frac{\dot{L}}{L}$ (black solid line) as functions of tissue length L. Shown on a log log plot. (F) Scaling error defined as: $\left|\frac{\partial\lambda}{\partial L}L\right|$ as a function of time. The scaling error is a dimensionless parameter describing the change in the sharpness of the gradient (λ) relative to the growth of the tissue. Excellent scaling is achieved when $\left|\frac{\partial\lambda}{\partial L}L\right|{<}1$.

Development (2014) 141, 2150-2156 doi:10.1242/dev.107011

Table 1. Scaling and uniform growth percentages

(A) **MDDR with ExR**	
Property	%
Final size	100
Scaling	98.5
Uniform growth	81
Scaling and uniform growth	80.4
(B) **MDDR**	
Property	%
Final size	100
Scaling	75
Uniform growth	100
Scaling and uniform growth	75

growth termination at final time. We verified that all three properties were observed over a wide range of parameters and were also observed for nonlinear morphogen degradation, absorptive boundary conditions and size-dependent Dpp flux (Table 1A; supplementary material Table S1 and Figs S11, S12). Including MDDR increased the robustness of scaling relative to the system in which growth was independent of morphogen signaling: it was now significantly easier to define parameters leading to scaling and uniform growth.

Morphogen-dependent cell division leads to scaling and uniform growth in the absence of an expander

We expected scaling to be established towards late growth, when proliferation slows down. We were therefore surprised to note that scaling and uniform growth were evident very early in the dynamics. In fact, the Dpp gradient scaled even at growth rates that were too rapid to enable efficient compensation by the ExR motif (supplementary material Fig. S2). This is in contrast to the situation of morphogen-independent growth, where scaling was lost in rapidly growing tissues (supplementary material Fig. S1). We therefore asked whether scaling can also be obtained in the absence of ExR feedback.

We simulated the morphogen dynamics in the absence of an expander. Strikingly, although no global feedback was present, this local dynamics was sufficient to reproduce the three global properties described above: scaling of the morphogen gradient with the size of the growing tissue (Fig. 3A,B,F), spatially uniform growth (Fig. 3C) and growth arrest at a finite size (Fig. 3D). While the sharpness of the gradient, as well as the final tissue size, were sensitive to model parameters, all three qualitative properties were observed for a wide range of parameters and were robust also for temporal and spatial noise in the division rule itself (Tables 1, 2; supplementary material Figs S4-S6, S8). In particular, MDDR also provided scaling when the morphogen decay rate was faster than tissue growth, $\alpha_M > q$, as is typical for developing tissues. The effects of the advection and dilution terms are important in the initial phases of growth corresponding to first to early second instar, setting the scaled exponential profile for the entire dynamics consistent with our analytical analysis below. Later during growth, morphogen degradation is dominant over dilution and advection, and the local growth law by itself maintains the scaled gradient (Fig. 3E; supplementary material Figs S13-S15).

Analytical derivation

Our simulation results demonstrated that the local coupling of cell division to morphogen signaling can by itself provide gradient scaling, spatially uniform growth, and a finite size without the ExR

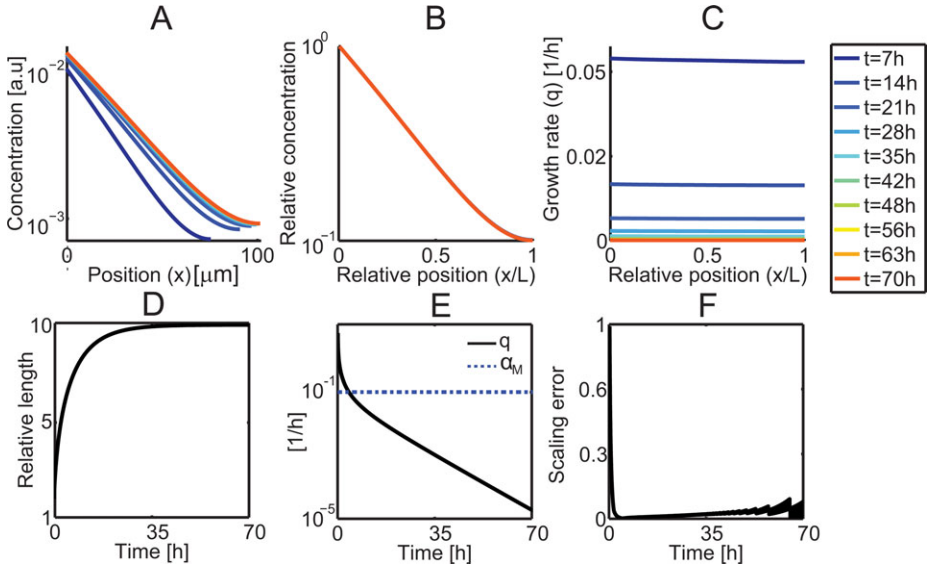

Fig. 3. Numerical simulation results for morphogen gradient dynamics in a tissue growing according to the MDDR without ExR feedback. In all cases, we assume a constant morphogen flux from the source. (A) Morphogen level as a function of position in the tissue at various times. (B) Relative morphogen level as a function of relative position in the tissue. Overlap of the profiles indicates scaling of morphogen gradient with size. (C) Proliferation rate at various times as a function of relative position. Growth is spatially uniform and its rate declines with time. (D) Fold change increase in tissue size as a function of time. (E) Morphogen degradation rate α (dashed blue line) and growth rate $q=\frac{\dot{L}}{L}$ (black solid line). Since there is no expander, morphogen degradation is constant. Note that scaling is achieved during most of the dynamics, when growth rate is much slower than morphogen degradation. (F) Scaling error defined as $\left|\frac{\partial\lambda}{\partial L}L\right|$ as a function of time. The scaling error is a dimensionless parameter describing the change in the sharpness of the gradient relative to the growth of the tissue. Excellent scaling is achieved when $\left|\frac{\partial\lambda}{\partial L}L\right|<1$.

Development (2014) 141, 2150-2156 doi:10.1242/dev.107011

Table 2. Sensitivity to model parameters

Parameter	MDDR	MDDR with ExR
(A) **Final size sensitivity**		
Morphogen diffusion coefficient (D_M)	0.31	0.22
Morphogen degradation rate (α_M)	0.31	0.35
Morphogen incoming flux (η)	0.02	0.01
Growth parameter (θ)	0.7	0.6
Initial tissue length (L_0)	0.3	0.2
(B) **Dynamics duration sensitivity**		
Morphogen diffusion coefficient (D_M)	0.13	0.15
Morphogen degradation rate (α_M)	0.07	0.02
Morphogen incoming flux (η)	0.036	0.035
Growth parameter (θ)	0.48	0.42
Initial tissue length (L_0)	0.31	0.15

mechanism. To better understand the origin of this behavior, we examined analytically the solution of Eqn 1 above, considering the scaled form of the morphogen profile observed numerically:

$$\frac{M(X,t)}{M(0,t)} = \hat{M}\left(\frac{X}{L}\right).$$

Assuming scaling of the gradient, together with the observation that the system converges to some steady state, implies that the resulting profile is exponential throughout the dynamics, following a short transient. This scaled solution further implies that the growth is uniform in space (see methods in the supplementary material for full derivation):

$$u_x = \frac{\dot{L}(t)}{L(t)}, \tag{4}$$

which is consistent with our simulation results. The scaled solution is then of the form (see methods in the supplementary material):

$$M(x,t) = \frac{\eta\lambda L(t)}{D_M}\exp\left(-\frac{1}{\lambda}\frac{x}{L(t)}\right), \tag{5}$$

$$L(t) = \sqrt{L_f^2(1-\exp(-\alpha_M t)) + L_0^2\exp(-\alpha_M t)},$$

$$L_f = \frac{1}{\lambda}\sqrt{\frac{D_M}{\alpha_M}}. \tag{6}$$

Here, λ is a dimensionless constant, defining the morphogen gradient length scale in the relative spatial coordinate $x/L(t)$. It depends on different parameters of the dynamics, including the initial length L_0 and θ (supplementary material Figs S5, S6). The only division rule consistent with this scaled solution is given by:

$$\frac{\dot{M}}{M} \approx \frac{\ln(2)}{\tau(t)} \tag{7}$$

when written in the coordinates of the moving cell. This solution is indeed consistent with the growth rule assumed in our simulations (Eq. 3), with θ=ln(2). As we saw in the simulations, choosing different θ values maintains the same qualitative behavior (Table 1B; see methods in the supplementary material for parameter values, Figs S8 and S10).

Taken together, this analytical result explains our numerical finding that MDDR can provide, by itself, gradient scaling, uniform growth and attainment of a finite size.

ExR feedback prolongs growth, increases tissue size and improves robustness

Next, we returned to the integrated system composed of both ExR and MDDR to examine whether the addition of ExR provides additional advantages. An extensive numerical screen revealed that scaling, uniform growth and finite tissue size are highly robust to the kinetic parameters of the system, both in the presence and absence of ExR feedback (Table 1). Final size and sharpness of the gradient were most sensitive to the growth parameter θ. Sensitivity to most parameters was reduced after introducing ExR (Table 2, Fig. 4A; supplementary material Figs S4 and S5). The percentage of scaled parameter sets increased with the addition of the expander, particularly in cases in which morphogen degradation was significantly faster than the typical cell cycle time (supplementary material Fig. S7).

To obtain analytical insight into the function of the expander in this integrated system, we approximated the ExR dynamics, Eqns 2a and 2b, assuming a flat expander profile. This is justified by previous analysis showing that ExR-dependent scaling requires a highly diffusible expander. Scaling together with a flat expander profile resulted in uniform tissue growth (see methods in the supplementary material). Further, we retrieve the exponential morphogen profile given by Eqn 5 as a solution to the coupled morphogen-expander system, with the temporal dynamics of the tissue length and expander concentration being specified by a system of ordinary differential equations (see methods in the

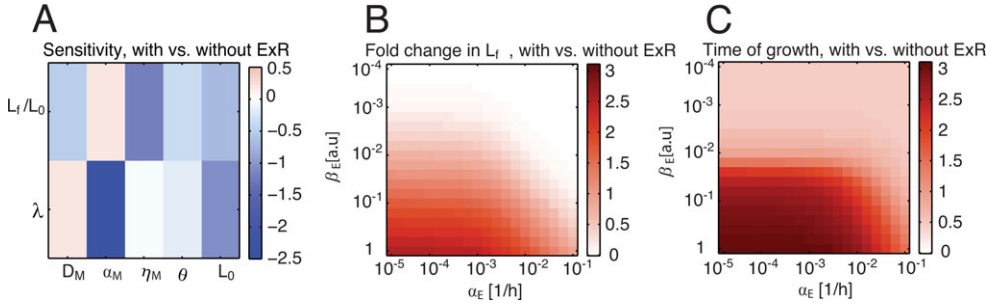

Fig. 4. ExR increases robustness, final size and prolongs growth. (A) Sensitivity log ratio of the final tissue size L_f and the gradient length scale λ, $\log_2\frac{S(p)_{\text{with ExR}}}{S(p)_{\text{No ExR}}}$, to various model parameters with versus without ExR. Sensitivity (S) of a quantity (X) to a parameter (p) is defined as the average over p of $\frac{p}{X}\left|\frac{\partial X}{\partial p}\right|$. In most cases, ExR improves robustness (blue shades). (B) The effect of expander degradation and production rates on $\log_2$ fold change in size: $\log_2\frac{(L_f/L_0)_{\text{with ExR}}}{(L_f/L_0)_{\text{No ExR}}}$. (C) The effect of the expander degradation and production rates on $\log_2$ fold change in growth duration (t_{ss}): $\log_2\frac{(t_{ss})_{\text{with ExR}}}{(t_{ss})_{\text{No ExR}}}$.

Development (2014) 141, 2150-2156 doi:10.1242/dev.107011

supplementary material, Eqs. 62 and 68). The resulting steady-state tissue length and expander concentration are given by:

$$E_f = \frac{c^*\beta_E}{\alpha_E}, \quad L_f = \frac{1}{\lambda}\sqrt{\frac{D_M}{\alpha_M}\left(1+\frac{c^*\beta_E}{\alpha_E}\right)}. \tag{8}$$

Here, c^* denotes the fraction of the tissue where the expander is expressed, which becomes constant following a short initial transient, once scaling commences (supplementary material Fig. S9). The morphogen and expander profiles are consistent with the cell division rule Eqn 7 (see methods in the supplementary material).

Eqn 8 suggests that the expander increases final tissue size. It also extends the time required to reach a steady state by reducing morphogen degradation rate, which is the dominant time scale in this system. This was indeed confirmed by our numerical screen: as predicted by Eqn 8, the fold increase in tissue length and in growth duration due to the addition of an ExR feedback depended on the typical expander level β_E/α_E (Fig. 4B,C). The fold increase in tissue size was also dependent on morphogen length scale at steady state (supplementary material Fig. S3):

$$\lambda_M = \sqrt{\frac{D_M}{\alpha_M}},$$

while the increase in growth duration was proportional to α_M, which is the morphogen degradation rate in the absence of the expander (supplementary material Fig. S3). Thus, removal of the expander from this integrated system is predicted to primarily affect the disc size and growth duration, while having a relatively low impact on the accuracy of scaling. This is in contrast to the experimental results obtained in the wing disc, when removal of *pentagone* resulted in a loss of scaling, but had a relatively minor effect on disc size (Ben-Zvi et al., 2011a, b; Hamaratoglu et al., 2011). This leads us to support the hypothesis that growth in the disc is not driven solely by Dpp signaling, as we discuss below.

DISCUSSION

The main result of the present study is the definition of a theoretical novel scaling mechanism that does not require global feedbacks but depends only on a local division rule, whereby cells divide when subject to some given increase in morphogen signaling. Previous studies have shown that this division rule leads to uniform growth, provided that the gradient scales by some other means (Wartlick et al., 2011). Here we show that, in fact, this division rule by itself can lead to morphogen gradient scaling. The simplicity of this growth rule, which depends only on local feedbacks, together with its robustness to the different parameters including those defining the growth rule itself, suggest that it might be employed during initial stages of tissue development when dynamics and growth are relatively fast and global feedbacks are harder to implement.

We identified the MDDR scaling mechanism while studying growth dynamics in the wing disc, where this morphogen-dependent growth rule was implicated in the context of the Dpp morphogen. We and others have recently shown that scaling of the Dpp morphogen in the wing disc depends on Pentagone, which is likely to function as the expander in the ExR mechanism (Ben-Zvi et al., 2011a; Hamaratoglu et al., 2011). We find that the integrated dynamics composed of both the ExR and the Dpp-dependent MDDR is consistent with many properties of the wing disc. Interestingly, it might also resolve an apparent limitation of the ExR in explaining the independent growth control of the anterior and posterior compartments of the wing disc: inhibition of Dpp signaling in one half of the disc does not substantially affect growth in the other half. This result appears incompatible with global feedback mechanisms, such as those proposed in ExR models. Interestingly, when simulating ExR dynamics combined with an early phase in which the MDDR is active, we find that it can in fact contribute to scaling at the two compartments independently (supplementary material Fig. S10).

In the context of the integrated dynamics, ExR functions primarily in extending the growth duration and increasing tissue size. Removing this feedback is predicted to reduce tissue size but not to alter scaling significantly. This, however, is not consistent with the findings in the wing disc, where removal of *pentagone* abolished scaling but resulted in only a minor reduction (~25%) in length of the AP axis of the disc. Therefore, either our model does not apply to the disc entirely, or it supports the hypothesis that at third instar growth is not entirely driven by the temporal increase in Dpp, and is defined either by absolute Dpp levels or by alternative signals as well (Schwank et al., 2011). If indeed the MDDR model applies to the wing disc, we expect during first and second instars that Dpp levels will correlate with cell division pattern and that scaling will persist in both wild-type and *pentagone* null wing discs. Notably, scaling of the Dpp gradient in wild type would still imply a correlation of cell division with the temporal increase in Dpp signaling (Wartlick et al., 2011), despite the lack of causality as shown by our analytical analysis.

To summarize, we propose that the morphogen-dependent growth rule may complement ExR feedback during wing disc growth, but is unlikely to be instructive for growth at late stages. More generally, our results suggest that a local coupling of cell division with morphogen signaling can establish global pattern scaling and tissue growth properties.

MATERIALS AND METHODS

Parameters

See methods in the supplementary material for full parameter lists.

Numerical method

In order to perform numerical simulations, we transform the morphogen evolution equation by $[x,t]\rightarrow[Y,t]$, with Y being the starting position of a cell at position x and time t. By setting $\bar{M}(Y,t) = M(x,t)$, $\bar{E}(Y,t) = M(x,t)$ the morphogen dynamics equation (Eqn 2) results in:

$$\bar{M}_t = \frac{D_M}{x_Y}\left(\frac{\bar{M}_Y}{x_Y}\right)_Y - \alpha(E)\cdot\bar{M} - \ln(2)\tau^{-1}(Y,t)\cdot\bar{M}, \tag{9}$$

$$\bar{E}_t = \frac{D_E}{x_Y}\left(\frac{\bar{E}_Y}{x_Y}\right)_Y - \alpha_E\cdot\bar{E} - \ln(2)\tau^{-1}(Y,t)\cdot\bar{E} + \beta_E\, h(\bar{M}), \tag{10}$$

$$\frac{dx_Y}{dt} = \ln(2)\tau^{-1}x_Y x_Y(0) = 1. \tag{11}$$

The growth law in Eqn 7 leads to the following equivalent growth law (see methods in the supplementary material for derivation) for the growth parameter θ:

$$\tau^{-1} = \frac{1}{\ln(2)+\theta}\left(\frac{D_M}{x_Y\bar{M}}\left(\frac{\bar{M}_Y}{x_Y}\right)_Y - \alpha(E)\right). \tag{12}$$

The above coupled system is solved numerically using an explicit finite difference scheme (see methods in the supplementary material) and the solutions are re-interpolated to the growing domain. All simulations are

Development (2014) 141, 2150-2156 doi:10.1242/dev.107011

performed using MATLAB (MathWorks). The numerical method is described in detail in methods in the supplementary material.

Acknowledgements
We thank Dr Shlomi Kotler, Dr Dann Huh, Mr Oren Raz, Prof. Benny Shilo and members of our group for fruitful discussions.

Competing interests
The authors declare no competing financial interests.

Author contributions
I.A., D.B.-Z. and S.M. developed the concepts, performed simulations and analytical calculations, analyzed the results and prepared the manuscript prior to submission. N.B. developed the concepts, analyzed the results and prepared the manuscript prior to submission.

Funding
This work was supported by the European Research Council and the Israel Science Foundation. N.B. is the incumbent of the Lorna Greenberg Scherzer Professorial Chair, and the Minerva Foundation. D.B.-Z. is supported by the HFSP long term postdoctoral fellowship and by the Rothschild and Fulbright postdoctoral fellowships. S.M is supported by the European Research Council.

Supplementary material
Supplementary material available online at
http://dev.biologists.org/lookup/suppl/doi:10.1242/dev.107011/-/DC1

References

Aegerter-Wilmsen, T., Aegerter, C. M., Hafen, E. and Basler, K. (2007). Model for the regulation of size in the wing imaginal disc of Drosophila. *Mech. Dev.* **124**, 318-326.
Affolter, M. and Basler, K. (2007). The Decapentaplegic morphogen gradient: from pattern formation to growth regulation. *Nat. Rev. Genet.* **8**, 663-674.
Barkai, N. and Ben-Zvi, D. (2009). 'Big frog, small frog'–maintaining proportions in embryonic development: delivered on 2 July 2008 at the 33rd FEBS Congress in Athens, Greece. *FEBS J.* **276**, 1196-1207.
Ben-Zvi, D. and Barkai, N. (2010). Scaling of morphogen gradients by an expansion-repression integral feedback control. *Proc. Natl. Acad. Sci. U.S.A.* **107**, 6924-6929.
Ben-Zvi, D., Shilo, B.-Z., Fainsod, A. and Barkai, N. (2008). Scaling of the BMP activation gradient in Xenopus embryos. *Nature* **453**, 1205-1211.
Ben-Zvi, D., Pyrowolakis, G., Barkai, N. and Shilo, B.-Z. (2011a). Expansion-repression mechanism for scaling the Dpp activation gradient in Drosophila wing imaginal discs. *Curr. Biol.* **21**, 1391-1396.
Ben-Zvi, D., Shilo, B.-Z. and Barkai, N. (2011b). Scaling of morphogen gradients. *Curr. Opin. Genet. Dev.* **21**, 704-710.
Bittig, T. (2008). *Morphogenetic Signaling in Growing Tissues*. Dresden: Institut für Theoretische Physik Fakultät Mathematik und Naturwissenschaften, Technische Universität.
Böhni, R., Riesgo-Escovar, J., Oldham, S., Brogiolo, W., Stocker, H., Andruss, B. F., Beckingham, K. and Hafen, E. (1999). Autonomous control of cell and organ size by CHICO, a Drosophila homolog of vertebrate IRS1-4. *Cell* **97**, 865-875.
Cheung, D., Miles, C., Kreitman, M. and Ma, J. (2011). Scaling of the Bicoid morphogen gradient by a volume-dependent production rate. *Development* **138**, 2741-2749.
Day, S. J. and Lawrence, P. A. (2000). Measuring dimensions: the regulation of size and shape. *Development* **127**, 2977-2987.
Gierer, A. and Meinhardt, H. (1972). A theory of biological pattern formation. *Kybernetik* **12**, 30-39.
Gregor, T., McGregor, A. P. and Wieschaus, E. F. (2008). Shape and function of the Bicoid morphogen gradient in dipteran species with different sized embryos. *Dev. Biol.* **316**, 350-358.
Hamaratoglu, F., de Lachapelle, A. M., Pyrowolakis, G., Bergmann, S. and Affolter, M. (2011). Dpp signaling activity requires pentagone to scale with tissue size in the growing Drosophila wing imaginal disc. *PLoS Biol.* **9**, e1001182.
Houchmandzadeh, B., Wieschaus, E. and Leibler, S. (2002). Establishment of developmental precision and proportions in the early Drosophila embryo. *Nature* **415**, 798-802.
Hufnagel, L., Teleman, A. A., Rouault, H., Cohen, S. M. and Shraiman, B. I. (2007). On the mechanism of wing size determination in fly development. *Proc. Natl. Acad. Sci. U.S.A.* **104**, 3835-3840.
Johnston, L. A. and Sanders, A. L. (2003). Wingless promotes cell survival but constrains growth during Drosophila wing development. *Nat. Cell Biol.* **5**, 827-833.
Kicheva, A., Pantazis, P., Bollenbach, T., Kalaidzidis, Y., Bittig, T., Julicher, F. and Gonzalez-Gaitan, M. (2007). Kinetics of morphogen gradient formation. *Science* **315**, 521-525.
Lanctot, A. A., Peng, C.-Y., Pawlisz, A. S., Joksimovic, M. and Feng, Y. (2013). Spatially dependent dynamic MAPK modulation by the Nde1-Lis1-Brap complex patterns mammalian CNS. *Dev. Cell* **25**, 241-255.
Milan, M., Campuzano, S. and Garcia-Bellido, A. (1996). Cell cycling and patterned cell proliferation in the Drosophila wing during metamorphosis. *Proc. Natl. Acad. Sci. U.S.A.* **93**, 11687-11692.
Patel, N. H. and Lall, S. (2002). Developmental biology: precision patterning. *Nature* **415**, 748-749.
Restrepo, S. and Basler, K. (2011). Morphogen gradients: expand and repress. *Curr. Biol.* **21**, R815-R817.
Rogulja, D. and Irvine, K. D. (2005). Regulation of cell proliferation by a morphogen gradient. *Cell* **123**, 449-461.
Rogulja, D., Rauskolb, C. and Irvine, K. D. (2008). Morphogen control of wing growth through the Fat signaling pathway. *Dev. Cell* **15**, 309-321.
Sato, M. and Kornberg, T. B. (2002). FGF is an essential mitogen and chemoattractant for the air sacs of the Drosophila Tracheal System. *Dev. Cell* **3**, 195-207.
Schwank, G. and Basler, K. (2010). Regulation of organ growth by morphogen gradients. *Cold Spring Harb. Perspect. Biol.* **2**, a001669.
Schwank, G., Restrepo, S. and Basler, K. (2008). Growth regulation by Dpp: an essential role for Brinker and a non-essential role for graded signaling levels. *Development* **135**, 4003-4013.
Schwank, G., Tauriello, G., Yagi, R., Kranz, E., Koumoutsakos, P. and Basler, K. (2011). Antagonistic growth regulation by Dpp and Fat drives uniform cell proliferation. *Dev. Cell* **20**, 123-130.
Schwank, G., Yang, S.-F., Restrepo, S. and Basler, K. (2012). Comment on "Dynamics of dpp signaling and proliferation control". *Science* **335**, 401.
Shraiman, B. I. (2005). Mechanical feedback as a possible regulator of tissue growth. *Proc. Natl. Acad. Sci. U.S.A.* **102**, 3318-3323.
Teleman, A. A. and Cohen, S. M. (2000). Dpp gradient formation in the Drosophila wing imaginal disc. *Cell* **103**, 971-980.
Towers, M., Mahood, R., Yin, Y. and Tickle, C. (2008). Integration of growth and specification in chick wing digit-patterning. *Nature* **452**, 882-886.
Vuilleumier, R., Affolter, M. and Pyrowolakis, G. (2011). Pentagone: patrolling BMP morphogen signaling. *Fly* **5**, 210-214.
Wartlick, O., Mumcu, P., Kicheva, A., Bittig, T., Seum, C., Julicher, F. and Gonzalez-Gaitan, M. (2011). Dynamics of Dpp signaling and proliferation control. *Science* **331**, 1154-1159.
Wartlick, O., Mumcu, P., Jülicher, F. and Gonzalez-Gaitan, M. (2012). Response to comment on "Dynamics of Dpp signaling and proliferation control". *Science* **335**, 401.
Wolpert, L. (1969). Positional information and the spatial pattern of cellular differentiation. *J. Theor. Biol.* **25**, 1-47.